# Comparative study of $HfN_x$ and Hf–Ge–N copper diffusion barriers on Ge

S. Rawal, E. Lambers, and D. P. Norton[a)]
*Department of Materials Science and Engineering, University of Florida, P.O. Box 116400, Gainesville, Florida 32611*

T. J. Anderson
*Department of Chemical Engineering, University of Florida, Gainesville, Florida 32611*

L. McElwee-White
*Department of Chemistry, University of Florida, Gainesville, Florida 32611*

(Received 25 February 2006; accepted 29 June 2006; published online 28 September 2006)

The diffusion barrier properties of $HfN_x$ and Hf–Ge–N thin films for Cu metallization on Ge are examined. The diffusion barrier films were deposited by reactive sputtering on *p*-Ge (001) single crystal substrates with varying thicknesses. Cu thin films were then deposited *in situ* on the diffusion barrier. The multilayer film structure was subsequently annealed in an Ar atmosphere. X-ray diffraction was used to determine the film crystallinity and identify intermetallic phases due to reactions involving the film and substrate. The $HfN_x$ and Hf–Ge–N diffusion barrier films remained amorphous for annealing temperatures up to 700 °C. At thickness of 50 nm, the $HfN_x$ films showed superior diffusion barrier properties as compared to Hf–Ge–N based on the appearance of secondary phases due to reactions and changes in the Cu morphology. These results suggest that $HfN_x$ is an effective barrier material for Cu integration on Ge. © *2006 American Institute of Physics*.
[DOI: 10.1063/1.2349470]

## INTRODUCTION

For many years, aluminum has been the primary interconnect metal for Si-based integrated circuits. However, with device dimensions shrinking to sub-45-nm and demands for high current density increasing, the conductivity and electromigration properties of Al become limitations to performance. In response, Cu is beginning to replace conventional Al interconnects given its better electromigration resistance and lower electrical resistance.[1–3] The use of low resistivity Cu compared to Al significantly reduces the circuit time constant delay, making the circuit faster. As the need for high speed electronics grows, there is also a renewed interest in Ge- and SiGe-based devices because of inherent advantages of Ge over Si, i.e., smaller $E_g$, higher mobility of charge carriers, and lower dopant activation energy.[4–6] $Si_{1-x}Ge_x$-based devices are also of interest because of the innate flexibility to tailor the band gap through the alloy composition.[7–9] These factors provide sufficient impetus to investigate barrier layer materials needed in incorporating Cu interconnects in $Si_{1-x}Ge_x$- and Ge-based devices.

For interconnect applications, copper cannot be deposited directly on Si–Ge since it diffuses rapidly in Si and Ge, creating deep level traps.[10,11] For the case of Si, it forms copper silicides at saturation. It also passivates dopants by forming Cu–*D* (*D* is a dopant atom) covalent pairs, thus altering the intended doping levels.[12] Copper is also known to diffuse rapidly in Ge with an average diffusion coefficient of $3\times10^{-5}$ $cm^2\,s^{-1}$ in the 700–900 °C temperature range.[13] Copper introduces three acceptor levels in Ge, two at $E_v+0.04$ and $E_v+0.32$ eV and another at $E_c-0.26$ eV, respectively.[14] Direct deposition of Cu on $Si_{1-x}Ge_x$ results in the formation of $Cu_3(Si_{1-x}Ge_x)$ and passivation of the dopants.[15] In addition to the above issues, Cu also exhibits poor adhesion to dielectrics commonly used in Si device structures.[16]

Considerable work has focused on identifying viable Cu diffusion barrier materials on Si. Since amorphous materials lack grain boundaries that are fast diffusion pathways, they are ideally suited for application as a diffusion barrier. Recent material systems that have been studied as possible Cu diffusion barriers for Si include refractory metal nitrides, such as TaN, TiN, and $WN_x$.[15,17–19] These binary nitrides, however, tend to recrystallize at moderate temperature, thus becoming susceptible to rapid Cu diffusion. There is significant interest in identifying diffusion barrier materials that remain amorphous at high processing temperature and effectively block Cu diffusion. Increasing the temperature necessary for crystallization can often be achieved by the addition of a third element to a binary matrix material. Some of the ternary material systems that have been studied include Ta–Si–N, W–Si–N, and W–Ge–N.[20–22] In this paper, we report on the recrystallization of $HfN_x$ and Hf–Ge–N thin films deposited on Ge and their diffusion barrier properties for Cu metallization.

## EXPERIMENTS

$HfN_x$ and Hf–Ge–N thin films with varying thicknesses (15, 50, and 300 nm) were deposited on *p*-Ge (001) single crystal substrates by reactive sputtering at room temperature. Prior to deposition, the substrates were cleaned with trichloroethylene, acetone, and methanol in an ultrasonic bath for 5 min each to remove any organic residue from the surface. The substrates were introduced in a reactive sputter deposi-

a)Author to whom correspondence should be addressed; electronic mail: dnort@mse.ufl.edu

 © 2006 American Institute of Physics

Downloaded 29 Sep 2006 to 128.227.61.27. Redistribution subject to AIP license or copyright, see http://jap.aip.org/jap/copyright.jsp

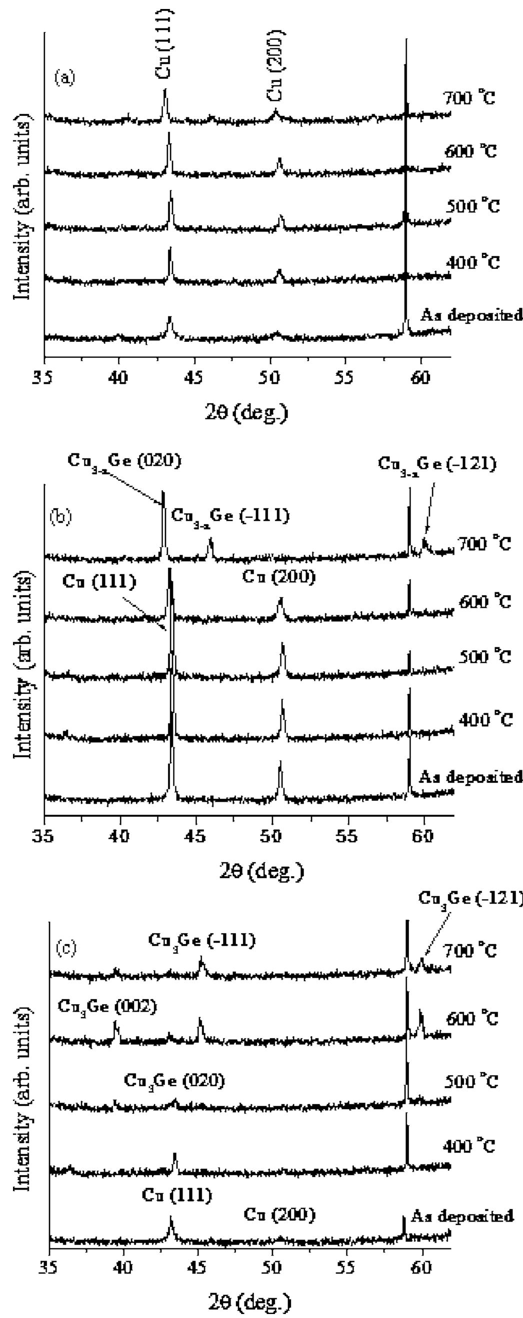


FIG. 1. X-ray diffraction patterns of $Cu/HfN_x/Ge$ films in as-deposited and annealed conditions for varying thicknesses of (a) 300 nm, (b) 50 nm, and (c) 15 nm.

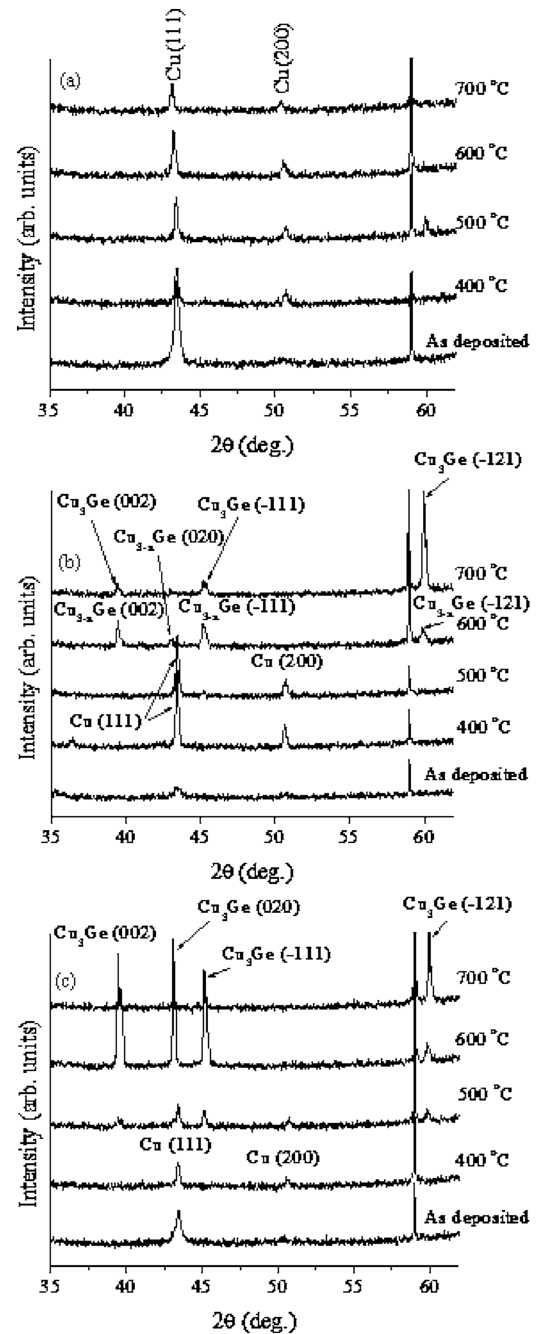


FIG. 2. X-ray diffraction patterns of Cu/Hf–Ge–N/Ge films in as-deposited and annealed conditions for varying thicknesses of (a) 300 nm, (b) 50 nm, and (c) 15 nm.

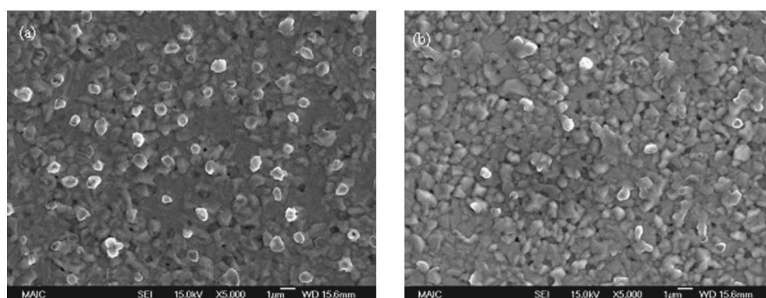

FIG. 3. FESEM images of 50 nm films annealed at 500 °C for 1 h: (a) $Cu/HfN_x/Ge$ and (b) Cu/Hf–Ge–N/Ge.

Downloaded 29 Sep 2006 to 128.227.61.27. Redistribution subject to AIP license or copyright, see http://jap.aip.org/jap/copyright.jsp

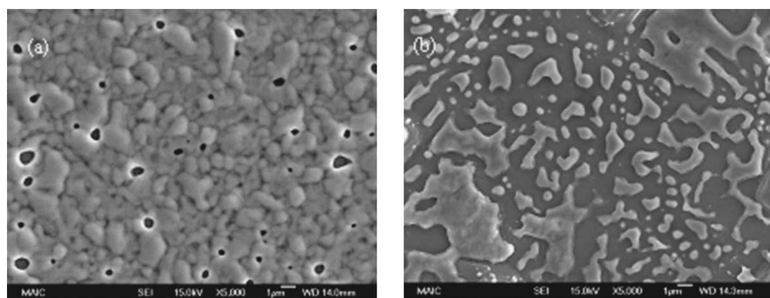

FIG. 4. FESEM images of 50 nm films annealed at 600 °C for 1 h: (a) Cu/$HfN_x$/Ge and (b) Cu/Hf–GeN/Ge.

tion chamber with a base pressure of $3\times10^{-7}$ Torr via a load lock. Nitrogen was incorporated in the film by flowing Ar and $N_2$ in the chamber at a ratio of 3:1. The total chamber pressure during deposition was 10 mTorr. Prior to deposition, the targets were cleaned *in situ* by presputtering with Ar+$N_2$ at a fixed chamber pressure of 15 mTorr. The forward sputtering powers for Hf and Ge were 200 and 100 W, respectively. The typical deposition rates for $HfN_x$ and Hf–Ge–N films were 1.8 and 6.23 nm/min, respectively. Identical thickness was achieved for both films by varying the deposition time. Film thickness was measured by a stylus profilometer.

Nitride film deposition was followed by *in situ* deposition of Cu films. The forward power used for Cu deposition was 200 W. The Cu thickness was maintained constant at 300 nm for all films. The deposition was carried out by flowing Ar inside the chamber at a fixed chamber pressure of 5 mTorr. Individual film stacks were then separately annealed in a tube furnace in the temperature range of 400–700 °C for 1 h. Before starting the annealing process, the tube was purged by flowing Ar gas at 65 SCCM for at least 10 h (SCCM denotes cubic centimeter per minute at STP). The film crystallinity before and after annealing was determined by x-ray diffraction (XRD) while the film surface morphology and roughness after annealing were determined by field emission scanning electron microscopy (FESEM). The chemical depth profile of Cu diffusion through the diffusion barrier was determined by energy dispersive spectroscopy (EDS). The chemical state analysis of Cu and intermetallic compound formation with Ge were investigated by x-ray photoelectron spectroscopy (XPS). Interface reactions and properties were determined by cross-section transmission electron microscopy (XTEM).

## RESULTS AND DISCUSSION

The $HfN_x$ films were amorphous in the as-deposited condition and showed no signs of recrystallization for any film thickness even after high temperature annealing. A lack of crystallization upon annealing is desirable as formation of grain boundaries leads to rapid Cu diffusion. The $HfN_x$ diffusion barrier properties are expected to be attractive based on their high melting temperature (3330 °C).[23] Materials that have a high melting temperature also generally show a high recrystallization temperature since both processes involve bond breaking. HfN films have been shown to be stable to thermal decomposition up to 1000 °C.[24] Figure 1 shows the x-ray diffraction patterns for Cu/$HfN_x$/Ge as deposited and after high temperature annealing in the range of 400–700 °C in an Ar atmosphere. For 300 and 50 nm thick $HfN_x$ diffusion barrier films that were annealed at a temperature of 600 °C or greater, the Cu films exhibit a shift in the Cu (111) peak towards smaller $2\theta$ values. This may indicate a reaction with the $HfN_x$ film. It is noted, however, that for the 300 nm thick $HfN_x$ barrier [Fig. 1(a)], no $Cu_3Ge$ phase was formed even after annealing at 700 °C. For the 50 nm thick $HfN_x$ film [Fig. 1(b)], as aforementioned, there is a definitive shift of Cu (111) peak at 700 °C annealing temperature which may be due to reaction of Cu with the underlying $HfN_x$ layer. Also evident for the 50 nm thick $HfN_x$ sample is the formation of nonstoichiometric $Cu_{3-x}Ge$ phase

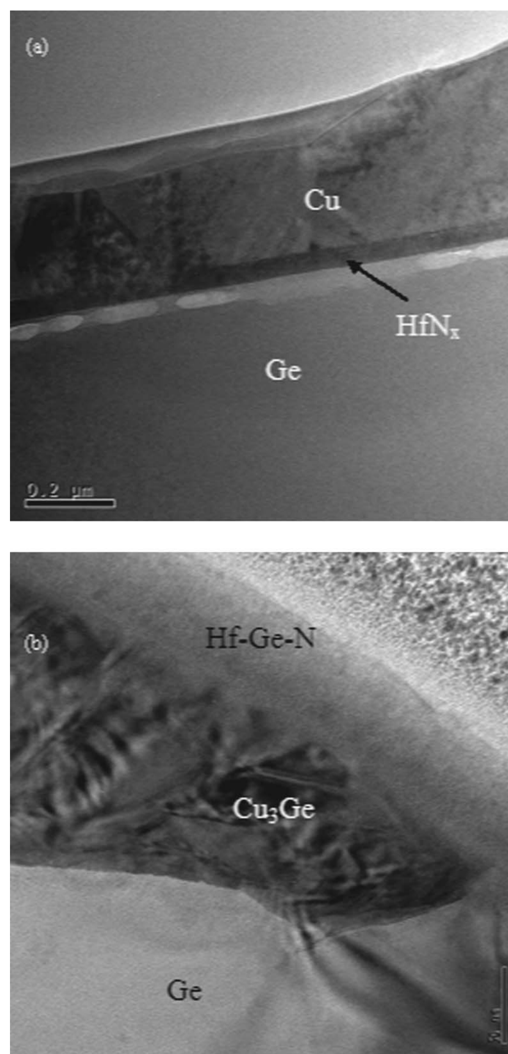


FIG. 5. XTEM images of 50 nm films annealed at 600 °C for 1 h: (a) Cu/$HfN_x$/Ge and (b) Cu/Hf–Ge–N/Ge.

Downloaded 29 Sep 2006 to 128.227.61.27. Redistribution subject to AIP license or copyright, see http://jap.aip.org/jap/copyright.jsp

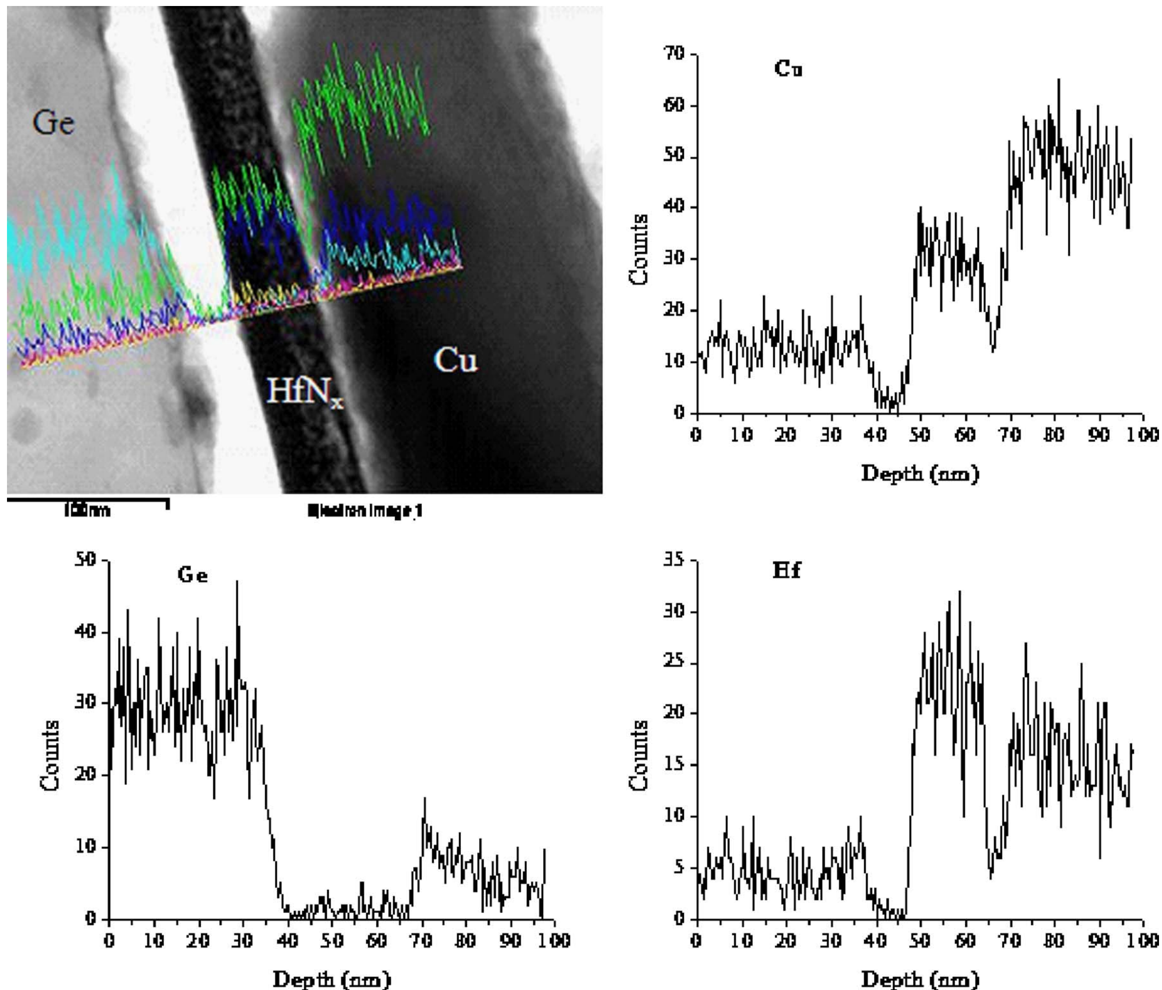


FIG. 6. EDS depth profile of 50 nm thick Cu/HfN$_x$/Ge annealed at 600 °C for 1 h.

after annealing at 700 °C. This indicates Cu diffusion through the HfN$_x$ diffusion barrier and reaction with the underlying Ge substrate. The Cu$_{3-x}$Ge phase could also have been formed by possible Ge outdiffusion through the diffusion barrier and subsequent reaction with Cu. For the ultrathin HfN$_x$ diffusion barrier film (15 nm), the barrier fails at lower temperature as is evident from Fig. 1(c) that shows Cu$_3$Ge phase formation after annealing at 500 °C and above. The 400 °C anneal pattern, however, does not reveal evidence of barrier failure.

The properties of Cu/Hf–Ge–N/Ge multilayers were then examined and compared to the Cu/HfN$_x$/Ge samples. Figure 2 shows x-ray diffraction patterns for Cu/Hf–Ge–N/Ge as deposited and after high temperature annealing in the range of 400–700 °C in Ar atmosphere. Based on the behavior of the thickest film, the Hf–Ge–N films remained amorphous after annealing at a temperature as high as 700 °C for all film thicknesses. For the 300 nm thick Hf–Ge–N film [Fig. 2(a)], there is little or no shift in the Cu (111) peak even after annealing at 700 °C. For the 50 nm thick Hf–Ge–N film [Fig. 2(b)], Cu$_{3-x}$Ge phase formation is evident after annealing at 600 °C, indicating that Cu has diffused through the barrier film to react with the underlying Ge substrate. It is also noted for the 600 °C annealed sample that the Cu (200) and (111) peaks are no longer present, suggesting significant loss of Cu to the underlying material. At 700 °C annealing temperature, sufficient Cu diffuses through the barrier layer to form stoichiometric Cu$_3$Ge phase, again indicating barrier failure.

These data suggest that while Hf–Ge–N and HfN$_x$ have similar recrystallization behavior, the diffusion barrier properties of HfN$_x$ are superior. In particular, the absence of the Cu (200) peak for the film on 50 nm thick Hf–Ge–N annealed at 600 °C suggests significant diffusion as compared to HfN$_x$.

One possible factor in determining the properties of the two materials relates to the relative percentages of the elements present in the diffusion barrier. As mentioned before, HfN$_x$ and Hf–Ge–N films were deposited at the rates of 1.8 and 6.23 nm/min, respectively. As the forwarding power to Hf was kept constant during deposition of both films, the total Hf content in the HfN$_x$ sample is about 3.5 times greater than that for the corresponding Hf–Ge–N film of the same thickness. This results in the deposition of a Ge-rich Hf–Ge–N film. Cu is known to react readily with Ge. For example, at room temperature, a 20 nm Cu$_3$Ge reaction layer will form at a Cu/Ge interface in 24 h in a binary reaction couple[25] and the reaction rate should increase with increased anneal temperature. The atomic percentages of each element present in Hf–Ge–N film as measured by Auger electron

Downloaded 29 Sep 2006 to 128.227.61.27. Redistribution subject to AIP license or copyright, see http://jap.aip.org/jap/copyright.jsp

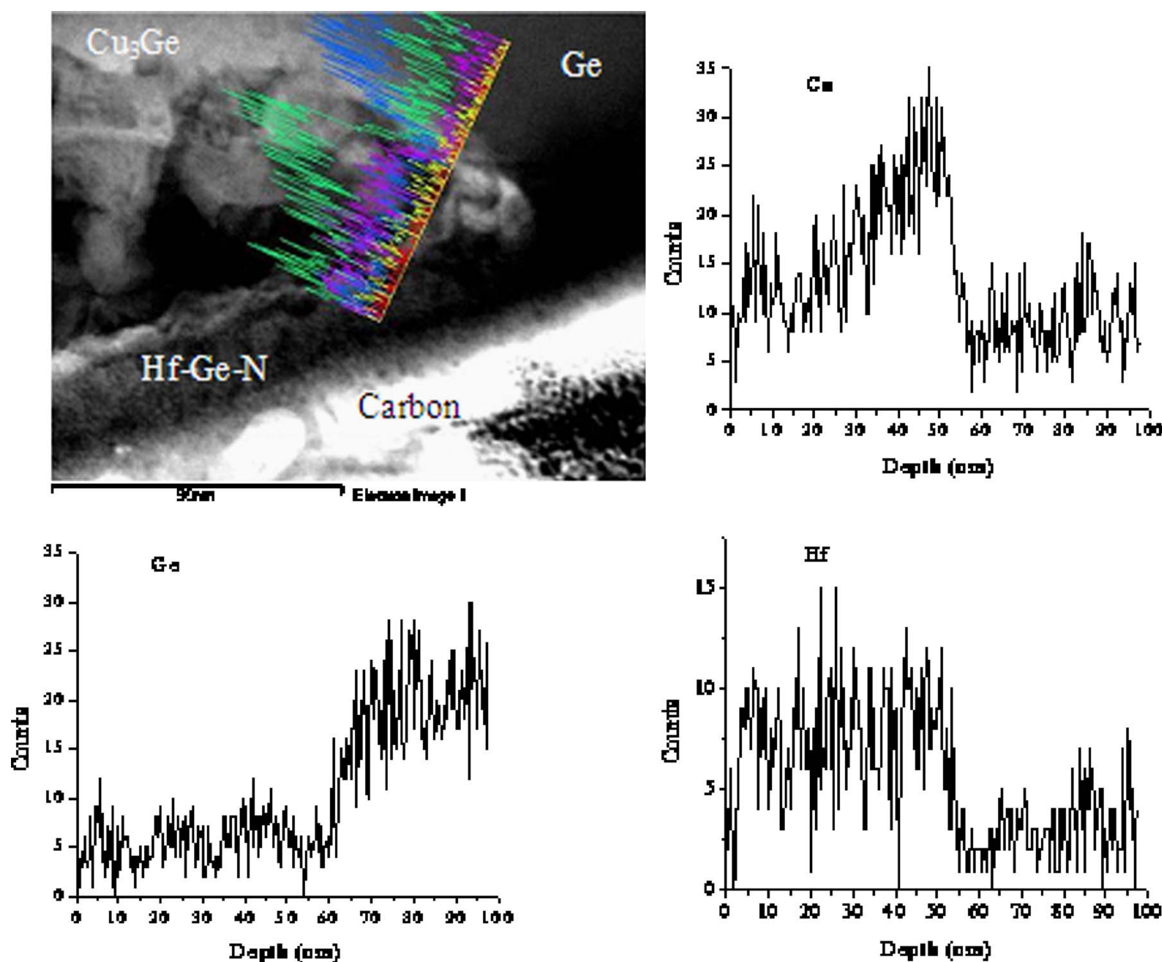


FIG. 7. EDS depth profile of 50 nm thick Cu/Hf–Ge–N/Ge annealed at 600 °C for 1 h.

spectroscopy were 3 at. % nitrogen, 41.5 at. % oxygen, 28.8 at. % germanium, and 26.7 at. % hafnium in as-deposited condition.

The surface morphology of the barrier materials was revealed by field emission scanning electron microscopy. Figure 3 shows a comparison of FESEM micrographs for (a) Cu/$HfN_x$/Ge and (b) Cu/Hf–Ge–N/Ge annealed at 500 °C; the samples retained barrier integrity as evidenced by the XRD patterns shown in Figs. 1(b) and 2(b). The thickness of each $HfN_x$ and Hf–Ge–N layers was 50 nm. The grain structure observed in the micrographs is that of the Cu. Note that there is no evidence of delamination. Figure 4 shows the FESEM micrographs for 50 nm thick (a) Cu/$HfN_x$/Ge and (b) Cu/Hf–Ge–N/Ge films annealed at 600 °C. After annealing at 600 °C, the surface morphology is significantly different for the copper films on $HfN_x$ as compared to that on Hf–Ge–N films. For Cu on the $HfN_x$, the Cu films are continuous with a roughness similar to that seen for the 500 °C anneal. For the Cu on Hf–Ge–N, however, significant Cu segregation is observed. This is consistent with the suppression of the (200) Cu peak for this structure and annealing temperature. Reaction with the Hf–Ge–N and possible Cu diffusion through the Hf–Ge–N film lead to depletion of Cu from the surface and segregation of Cu islands in the [111] direction. This apparent Cu loss on the surface is in agreement with the XRD data showing the appearance of $Cu_3Ge$ peaks for Cu films on Hf–Ge–N barriers that are annealed at 600 °C. No such peaks are detected for the comparative $HfN_x$ film, suggesting improved diffusion barrier quality of the latter film.

The interface properties and reactions were examined by cross-section transmission electron microscopy. Figure 5 shows the XTEM images of the 50 nm thick (a) Cu/$HfN_x$/Ge and (b) Cu/Hf–Ge–N/Ge films after annealing at 600 °C for 1 h. Cu diffusion is clearly seen in the Hf–Ge–N film with the formation of $Cu_3Ge$ phase below the diffusion barrier film. The image of the $HfN_x$ film, however, shows a negligible amount of Cu diffusion as indicated by a continuous Cu film on the surface and no indication of formation of the $Cu_3Ge$ phase. The discontinuous layer at the $HfN_x$/Ge interface is due to delamination of $HfN_x$. This could be due to TEM sample preparation by focused ion beam (FIB). The chemical diffusion profile of Cu was determined by energy dispersive spectroscopy attached to the cross-section TEM. Figures 6 and 7 show the chemical diffusion profiles of Cu after annealing at 600 °C for 1 h for the $HfN_x$ and Hf–Ge–N films, respectively. A Cu signal is present in the Hf–Ge–N barrier layer and $Cu_3Ge$ has clearly formed by transport through the barrier film to the Ge substrate. In contrast, $HfN_x$ shows that little Cu signal is seen from the Ge substrate, indicating that the $HfN_x$ barrier layer prevented Cu diffusion to the Ge substrate. The EDS peak

Downloaded 29 Sep 2006 to 128.227.61.27. Redistribution subject to AIP license or copyright, see http://jap.aip.org/jap/copyright.jsp

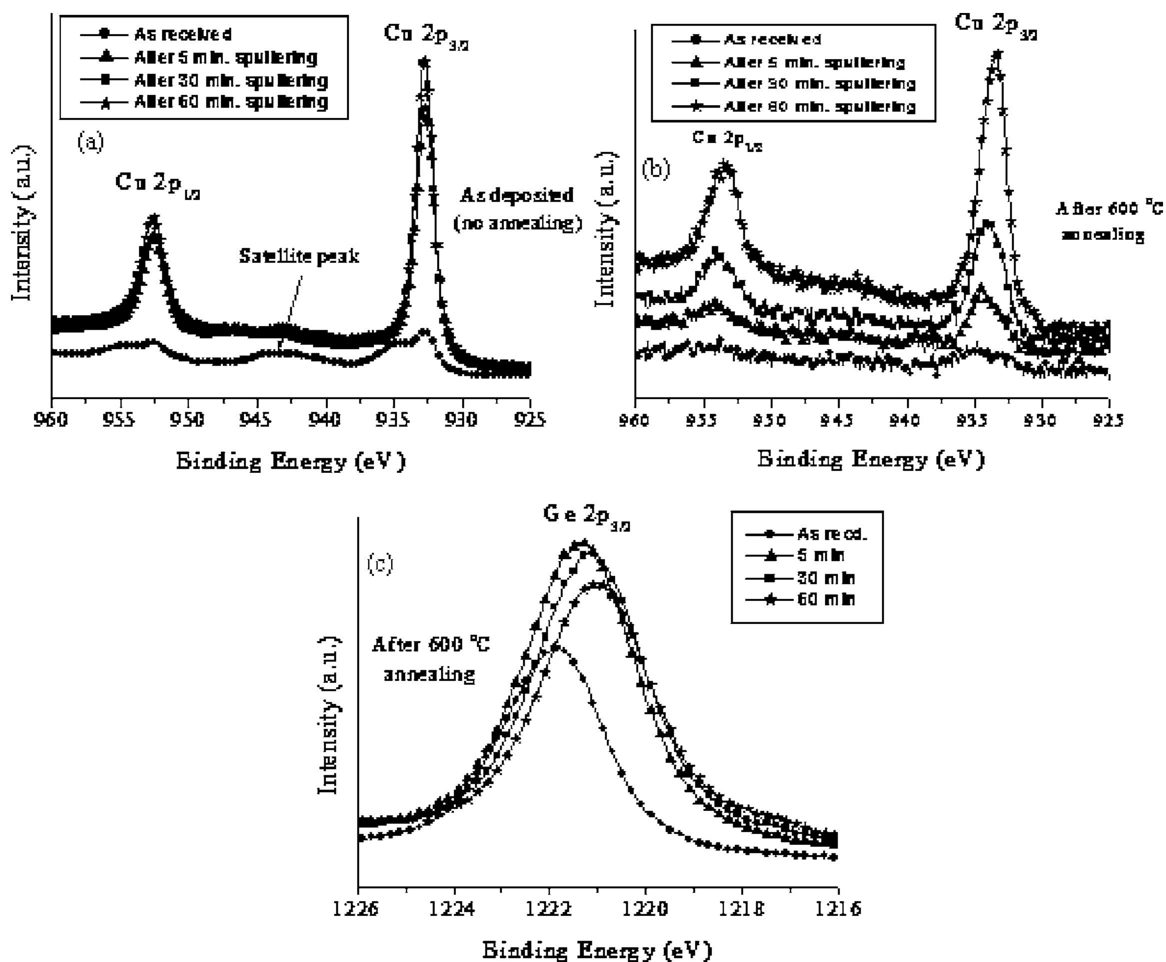


FIG. 8. XPS chemical state data at various sputtering times for 50 nm thick film of Cu/Hf–Ge–N/Ge for Cu 2*p* peak (a) in as-deposited condition and (b) annealed at 600 °C for 1 h, and (c) for Ge 2*p* peak annealed at 600 °C for 1 h.

positions of Cu and Hf overlap each other. As a result, a bump in the Cu intensity profile is observed in the $HfN_x$ layer. Also, a strong Hf EDS intensity is seen from the entire region of the Cu layer due to the EDS detector's inability to differentiate between Cu and Hf.

The chemical state of Cu and intermetallic phase formation after annealing were determined by XPS. Figure 8 compares the Cu $2p_{3/2}$ peak shifts in Cu/Hf–Ge–N/Ge film for different sputtering times (a) in the as-deposited material and (b) after annealing the film at 600 °C for 1 h and (c) Ge $2p_{3/2}$ peak shifts in Cu/Hf–Ge–N/Ge for different sputtering times after annealing at 600 °C for 1 h. The Cu surface of the as-deposited film is clearly oxidized, forming a CuO layer. This is evident from the characteristic satellite peaks formed for $Cu^{+2}$. After sputtering, however, the peak shifts and matches with pure Cu (932.8 eV). As seen in Fig. 8(b), after annealing the 50 nm Cu/Hf–Ge–N film at 600 °C, the Cu $2p_{3/2}$ peak in the as-received condition forms at 934.8 eV, indicating its reaction with Ge and formation of $Cu_{3-x}Ge$. This is also consistent with the XRD and XTEM data which show the formation of $Cu_{3-x}Ge$. The peak intensity increases with sputtering time as more Cu participation in the Cu–Ge bond is revealed. Apparently, there is a slight shift in the Cu $2p_{3/2}$ peak to 933.3 eV after 60 min sputtering, indicating that Cu might react with oxygen and form a Cu–O compound. The Ge $2p_{3/2}$ peak appears at 1221.9 eV after annealing at 600 °C. The Ge $2p_{3/2}$ peak intensity increases with sputtering time, indicating increased Ge participation in the Cu–Ge bond formation. There is a shift in the Ge $2p_{3/2}$ peak position to 1221 eV after sputtering for 60 min. This might be due to reaction with oxygen and formation of Ge–O bond.

## CONCLUSIONS

In conclusion, a comparative study of the diffusion barrier properties of Hf–Ge–N and $HfN_x$ deposited on (001) Ge single crystal wafers was conducted. The FESEM images show almost identical surface morphology of Cu films after annealing at 500 °C. Annealing at 600 °C, however, results in considerable extent of diffusion across the Hf–Ge–N films, leaving a discontinuous Cu film on the surface. Furthermore, sufficient Cu transport occurs to form $Cu_3Ge$ which is evident from XRD data. In contrast, little or no diffusion takes place for $HfN_x$ films of the same 50 nm thickness and annealing condition, leaving Cu films continuous and smoother. This is also substantiated by cross-sectional TEM images which clearly show the formation of a $Cu_3Ge$ phase below the Hf–Ge–N diffusion barrier, but no such phase is formed in the comparative $HfN_x$ film after annealing

Downloaded 29 Sep 2006 to 128.227.61.27. Redistribution subject to AIP license or copyright, see http://jap.aip.org/jap/copyright.jsp

at 600 °C. The chemical valence state was determined by XPS and the results point to Cu–Ge bond formation after high temperature annealing. The chemical diffusion profile measured by EDS shows Cu signal emanating from the Hf–Ge–N diffusion barrier and the underlying $Cu_3Ge$ phase that formed after annealing at 600 °C. There is little or no Cu signal, however, observed in the $HfN_x$ diffusion barrier and underlying Ge substrate, indicating that the $HfN_x$ diffusion barrier was successful in preventing Cu diffusion to the substrate. It is thus concluded that $HfN_x$ is an attractive diffusion barrier for Cu on Ge, while Hf–Ge–N demonstrates limited utility.

## ACKNOWLEDGMENTS

The above work was supported by the National Science Foundation under Grant No. CHE-0304810. The authors would like to acknowledge the Major Analytical Instrumentation Center (MAIC), Department of Materials Science and Engineering, University of Florida where all characterizations were carried out. The authors would also like to thank Ivan Kravachenko and Bill Lewis at the University of Florida Nanofabrication Facility for their help with sputtering and Kerry Siebein, MAIC, University of Florida for assistance with EDS and XTEM.

[1] R. J. Gutmann, T. P. Chow, A. E. Kaloyeros, W. A. Lanford, and S. P. Muraka, Thin Solid Films **262**, 177 (1995).
[2] N. Awaya, H. Inokawa, E. Yamamoto, Y. Okazaki, M. Miyake, Y. Arita, and T. Kobayashi, IEEE Trans. Electron Devices **43**, 8 (1996).
[3] Y. Igarashi, T. Yamanobe, and T. Ito, Thin Solid Films **262**, 124 (1995).
[4] H. Shang *et al.*, IEEE Electron Device Lett. **25**, 135 (2004).
[5] O. C. Chi and K. C. Saraswat, Proceedings of the International Conference on Integrated Circuit Design Technology, 2004 (unpublished), p. 245.
[6] O. C. Chi, K. Gopalakrishnan, P. B. Griffin, J. D. Plummer, and K. C. Saraswat, Appl. Phys. Lett. **83**, 3275 (2003).
[7] J. D. Cressler, IEEE Trans. Microwave Theory Tech. **46**, 572 (1998).
[8] D. J. Paul, Thin Solid Films **321**, 172 (1998).
[9] T. E. Whall and E. H. C. Parker, J. Phys. D **31**, 1397 (1998).
[10] S. M. Sze, *VLSI Technology*, 2nd ed. (McGraw-Hill, New York, 1988), pp. 307 and 308.
[11] E. Simoen, P. Clauws, M. Lamon, and J. Vennik, Semicond. Sci. Technol. **1**, 53 (1986).
[12] M. O. Aboelfotoh and B. G. Svenson, Phys. Rev. B **44**, 12742 (1991).
[13] C. S. Fuller, J. D. Struthers, J. A. Ditzenberger, and K. B. Wolfstirn, Phys. Rev. **93**, 1182 (1954).
[14] H. H. Woodbury and W. W. Tyler, Phys. Rev. **105**, 84 (1957).
[15] M. Barthula, M. O. Aboelfotoh, and F. Meyer, Microelectron. Eng. **55**, 323 (2001).
[16] B. S. Kang, S. M. Lee, J. S. Kwak, D. S. Yoon, and H. K. Baik, J. Electrochem. Soc. **144**, 1807 (1997).
[17] S. W. Loh, D. H. Zhang, C. Y. Li, R. Liu, and A. T. S. Wee, Thin Solid Films **462–463**, 240 (2004).
[18] J. Baumann, T. Werner, A. Ehrlich, M. Rennau, Ch. Kaufmann, and T. Gessner, Microelectron. Eng. **37–38**, 221 (1997).
[19] K. S. Lee, Jpn. J. Appl. Phys., Part 1 **42**, 3368 (2003).
[20] R. Hubner *et al.*, Thin Solid Films **468**, 183 (2004).
[21] S. Bystrova, J. Holleman, and P. H. Woerlee, Microelectron. Eng. **55**, 189 (2001).
[22] S. Rawal, D. P. Norton, T. J. Anderson, and L. McElwee-White, Appl. Phys. A: Mater. Sci. Process. (submitted).
[23] M. Wittmer, J. Vac. Sci. Technol. A **3**, 1797 (1985).
[24] H. Y. Yu *et al.*, IEEE Electron Device Lett. **24**, 230 (2003).
[25] L. Krusin and M. O. Aboelfotoh, Appl. Phys. Lett. **58**, 1341 (1991).

**Downloaded 29 Sep 2006 to 128.227.61.27. Redistribution subject to AIP license or copyright, see http://jap.aip.org/jap/copyright.jsp**